Dyes and Pigments 147 (2017) 537–543

Contents lists available at ScienceDirect

Dyes and Pigments

journal homepage: www.elsevier.com/locate/dyepig

Alkyl length dependent reversible mechanofluorochromism of phenothiazine derivatives functionalized with formyl group

Junhui Jia*, Yuying Wu

Key Laboratory of Magnetic Molecules and Magnetic Information Material, Ministry of Education, The School of Chemical and Material Science, Shanxi Normal University, Linfen, 041004, PR China

ARTICLE INFO

Article history:
Received 10 May 2017
Received in revised form
3 August 2017
Accepted 27 August 2017
Available online 30 August 2017

Keywords:
Phenothiazine
Mechanofluorochromism
Chain length-dependent

ABSTRACT

A series of D-A typed phenothiazine derivatives functionalized by formyl group (PCAn, n = 1, 2, 4 and 6) with different lengths of *N*-alkyl chains have been designed and synthesized to systematically investigate the effect of chain length on their solid-state fluorescence properties. The results showed that these compounds emitted strong fluorescence in solutions and solid states with 52%, 42%, 49% and 45% solid-state absolute fluorescence quantum yield (Φ_F), respectively. Their emission wavelengths were strongly affected by solvent polarity, indicating intramolecular charge transfer (ICT) transitions. Interestingly, PCAn solids exhibit not only naked-eye visible and reversible mechanochromic behavior, but chain length-dependent emission properties. **PCA1** shows smaller fluorescence spectrum shifts (22 nm) under mechanical force stimuli. Homologs with longer alkyl chains exhibit similar mechanochromic behaviors but larger fluorescence contrasts after grinding except for **PCA6**. Moreover, the fluorescence emission of ground solid **PCA1** and **PCA4** can recover at room temperature, **PCA2** need high temperatures for fluorescence to be restored, and XRD and DSC revealed that the transformation between crystalline and amorphous states upon various external stimuli was responsible for the MFC behavior. This work demonstrates the feasibility of tuning the solid-state optical properties of fluorescent organic compounds by combining the simple alteration of chemical structure and the physical change of aggregate morphology under external stimuli.

1. Introduction

Smart conjugated luminescent materials have attracted a great deal of attention due to their multi-stimuli responsive emission characteristics and broad applications in the fields of molecular probes, organic light-emitting devices (OLED), optical data recording and data security protection. Particularly, dynamic altering and switching of solid-state luminescence of organic materials upon light, heat, pressure or other external factors, is attracting a lot of interest. Especially, some fluorescent organic molecules can alter their luminescent properties in response to external mechanical stimuli such as shearing, grinding, or pressing, which is known as mechanofluorochromism (MFC) [1–4]. As a kind of "smart material," MFC compounds have attracted significant attention because of their promising applications in pressure sensors, optical storage, rewritable media, and security ink [5–8]. These fluorescent organic molecules can give changes in the color of their fluorescence under mechanical stress and be restored to their original state by annealing or fuming with solvent vapor instead of the chemical alteration of molecular structures [9–14]. However, MFC materials have started to draw increasing research attention only within the past few years and the types of MFC materials and in-depth understanding of MFC phenomena are limited. To date, many kinds of organic molecules have been exploited to show MFC properties [15–19]. Especially, some nonplanar π-conjugated fluorescent molecules, such as tetraphenylethene (TPE), 9,10-divinylanthracene, triphenylamine (TPA) derivatives and organoboron compounds, were preferentially considered to act as MFC materials, and interestingly, some D-π-A emissive molecules always contribute to the realization of fluorescence change under mechanical stimuli [20–31]. It is worth mentioning that phenothiazine was usually introduced to construct organic luminescent materials as an excellent functional blocks [32,33]. It has a nonplanar, bowl-shaped configuration, and recently some studies have found that it can be introduced into molecular structures to obtain MFC-active fluorescent molecules [34,35].

* Corresponding author.
E-mail address: jiajunhui@sxnu.edu.cn (J. Jia).

http://dx.doi.org/10.1016/j.dyepig.2017.08.049
0143-7208/

As is well known the alkyl length can influence molecular conformations, and change intermolecular interactions and even packing mode in solid states, which result in different MFC properties. However, the studies on the effects of alkyl length on MFC materials are limited owing to the scarcity of MFC materials and the mechanism is still unclear [36,37]. Therefore, there is still a great challenge for designing and synthesizing new MFC materials, as well as the accumulation of knowledge of the relationships between molecular structures and properties. In this context, much more systematic molecular design and structure-property investigation on MFC materials are becoming very necessary. To further understand the effect of alkyl chains on the solid-state fluorescence and mechanochromic luminescence, in the current work, we have prepared a series of phenothiazine derivatives functionalized with benzoyl group (PCAn, n = 1, 2, 4 and 6) with different lengths of *N*-alkyl chains (Scheme 1), and their photophysical properties and MFC behaviors were investigated in detail. The results showed that these molecules exhibited different MFC activities and their fluorescence emission and MFC behaviors are alkyl length-dependent.

2. Experimental section

2.1. General information

All the raw materials were used without further purification. All the analytical pure solvents were purchased from Beijing Chemical Works (Beijing, China). ^{1}H NMR and ^{13}C NMR spectra were recorded with a Mercury Plus instrument at 600 MHz and 151 MHz by using $CDCl_3$ as the solvent in all cases. High resolution mass spectra were performed on AB SCIEX Triple TOF™ 5600$^+$ LC-MS/MS series. FT-IR spectra were recorded with a Varian 660-IR FT-IR spectrometer by incorporation of samples into KBr disks. The UV–vis absorption spectra were obtained using a VARIAN Cary 5000 spectrophotometer. Photoluminescence measurements were obtained on a Cary Eclipse fluorescence spectrophotometer. The fluorescence quantum yields of PCAn (n = 1, 2, 4, and 6) in various solvents were measured by comparing with a standard (quinine in 0.1 N H_2SO_4, $\Phi_F = 0.546$) and the excitation wavelength was 365 nm. The solid fluorescence quantum yields were measured using an Edinburgh Instrument FLS920 with integrating cavity scanning (ICS) method. Cyclic voltammogram was performed using CHI 604B electrochemical workstation and measurement was carried out in dry CH_2Cl_2 with a scan rate at 100 mV/s. Three electrode configurations were used for the measurement: a platinum button was used as the working electrode, a platinum wire as the counter electrode, and Ag/AgCl as the reference electrode. The solution of Bu_4NBF_4 in DCM (0.1 M) was used as the supporting electrolyte. C, H, and N elemental analyses were performed with a vario MACRO cube elemental analyzer. The XRD patterns were obtained on an Empyrean X-ray diffraction instrument equipped with graphite-monochromatized Cu Kα radiation (λ = 1.5418 Å) by employing a scanning rate of 0.026° s^{-1} in the 2θ range from 5 to 50. Differential scanning calorimetry (DSC) curves were obtained on a DSC 200 F3 at a heating rate of 10 °C min^{-1}, and the data of all samples (pristine and ground) were collected when they were heated for the first time. Pressing experiment: A quantity of PCAn and KBr powder was simply mixed in a mortar and then pressed with IR pellet press for 1 min at room temperature under the pressure of 1500 psi. Annealing experiment: The pressed sample was put into an oven whose temperature was 30 °C over Tc (cold-crystallization temperature of each compound) for 3 min. Solvent-fuming experiment: The ground sample was placed above the dichloromethane level and was exposed to the vapor for 1 min at room temperature. The molecular configuration was used to obtain the frontier orbitals of PCAn by density functional theory (DFT) calculations at the B3LYP/6-31G (d, p) level with the Gaussian 09W program package.

2.2. Synthesis, procedures, and characterization

Compounds **1** and target compounds PCAn were synthesized by the reported methods [32,33], and the synthetic routes were shown in Scheme 2.

2.2.1. 10-Methyl-10H-phenothiazine-3-carbaldehyde (*PCA1*)

1.3 mL $POCl_3$ (16 mmol) was added into 2 mL DMF in 25 mL flask under ice-water bath, after being stirred for 10 min at room temperature, 10-methyl-10*H*-phenothiazine (1.7 g, 8 mmol) dissolved in 1, 2-dichloroethane (10 mL) was added into the above mixture drop-wise under ice-water bath, and then the resulting mixture was heated to reflux for 12 h. The reaction mixture was cooled to room temperature and poured into ice-water. The organic layer was extracted with dichloromethane and the combined organic layers were washed with saturated brine solution and water, and dried over anhydrous magnesium sulfate. After filtration and solvent evaporation, the residue was purified by silica-gel column chromatography using petroleum ether/dichloromethane (v:v = 1:1) as eluent, yellow-green solid was obtained after recrystallization from dichloromethane and diethyl ether. Yield: 0.96 g, 50%. mp: 88–90 °C. IR (KBr, cm^{-1}): 1676, 1600, 1568, 1464, 1396, 1380, 1328, 1256, 1204, 752. ^{1}H NMR (600 MHz, $CDCl_3$) δ 9.81 (1 H, s), 7.66 (1 H, dd, J_1 = 1.8 Hz, J_2 = 1.8 Hz), 7.60 (1 H, d, J = 1.8 Hz), 7.21–7.18 (1 H, m), 7.14–7.12 (1 H, m), 7.00–6.98 (1 H, m), 6.85 (2 H, t, J = 8.2 Hz), 3.43 (3 H, s) (Fig. S1). ^{13}C NMR (151 MHz, $CDCl_3$) δ 190.09, 151.11, 144.13, 131.22, 130.46, 127.99, 127.78, 127.42, 127.32, 127.15, 124.03, 123.65, 122.59, 122.44, 114.78, 114.06, 113.72, 77.23, 77.02, 76.80, 35.84. (Fig. S2); MS (HR-MS): *m/z* 242.0537 [M+H]$^+$ (Fig. S3, Calcd for $C_{14}H_{11}NOS$: 241.0561); Anal. Calcd. (%) for $C_{14}H_{11}NOS$: C, 69.68; H, 4.59; N, 5.80. Found (%): C, 69.72; H, 4.61; N, 5.77.

2.2.2. 10-Ethyl-10H-phenothiazine-3-carbaldehyde (*PCA2*)

The synthetic method for compound **PCA2** was similar to that of compound **PCA1**. It was purified by column chromatography (silica gel, petroleum ether/CH_2Cl_2 = 1/1) to give yellow solid (49% in yield). mp: 100–101 °C. IR (KBr, cm^{-1}): 1672, 1600, 1576, 1468, 1398,

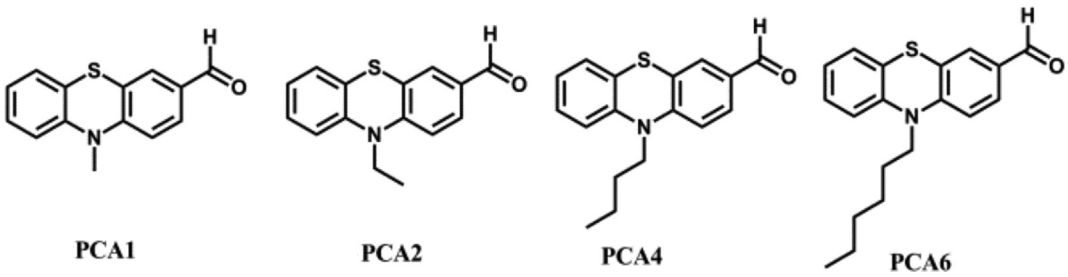

Scheme 1. The structures of **PCA1**, **PCA2**, **PCA4** and **PCA6**.

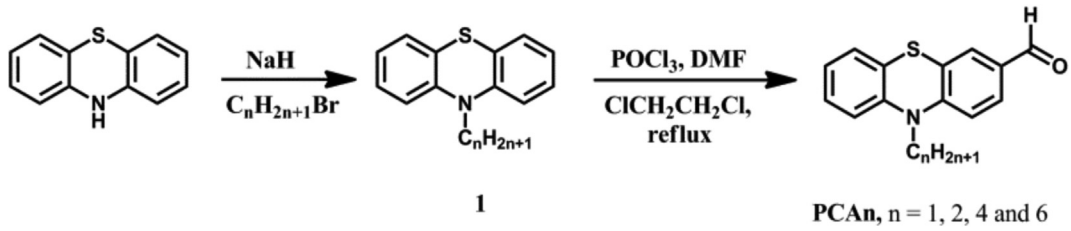

Scheme 2. Synthetic routes of **PCA1**, **PCA2**, **PCA4** and **PCA6**.

1368, 1325, 1256, 1240, 1200, 756. ^{1}H NMR (600 MHz, $CDCl_3$) δ 9.79 (1 H, s), 7.64–7.62 (1 H, dd, J_1 = 8.4 Hz, J_2 = 1.9 Hz), 7.57 (1 H, d, J = 1.9 Hz), 7.18–7.14 (1 H, m), 7.10 (1 H, dd, J_1 = 7.6 Hz, J_2 = 1.5 Hz), 6.98–6.94 (1 H, m), 6.90 (2 H, t, J = 8.0 Hz), 3.98 (2 H, m), 1.45 (3 H, t, J = 7.0 Hz) (Fig. S4). ^{13}C NMR (151 MHz, $CDCl_3$) δ 190.01, 150.30, 143.08, 131.01, 130.17, 128.26, 127.59, 127.49, 124.47, 123.55, 123.27, 115.57, 114.39, 77.23, 77.02, 76.81, 42.47, 12.87. (Fig. S5); MS (HR-MS): *m/z* 256.0579 $[M+H]^+$ (Fig. S6, Calcd for $C_{15}H_{13}NOS$: 255.0718); Anal. Calcd. (%) for $C_{15}H_{13}NOS$: C, 70.56; H, 5.13; N, 5.49. Found (%): C, 70.62; H, 5.11; N, 5.53.

2.2.3. 10-Butyl-10H-phenothiazine-3-carbaldehyde (*PCA4*)

The synthetic method for compound **PCA4** was similar to that of compound **PCA1**. It was purified by column chromatography (silica gel, petroleum ether/CH_2Cl_2 = 1/1) to give yellow solid (48% in yield). mp: 54–55 °C. IR (KBr, cm^{-1}): 1676, 1600, 1576, 1564, 1472, 1448, 1440, 1368, 1252, 1228, 1200, 752. ^{1}H NMR (600 MHz, $CDCl_3$) δ 9.79 (1 H, s), 7.65–7.63 (1 H, dd, J_1 = 8.4 Hz, J_2 = 1.9 Hz), 7.58 (1 H, d, J = 1.9 Hz), 7.18–7.15 (1 H, m), 7.12–7.10 (1 H, dd, J_1 = 7.6 Hz, J_2 = 1.5 Hz), 6.98–6.95 (1 H, m), 6.91–6.88 (2 H, dd, J_1 = 11.0 Hz, J_2 = 8.0 Hz), 3.91–3.88 (2 H, t, J = 6.0 Hz), 1.83–1.78 (2 H, m), 1.50–1.44 (2 H, m), 0.97–0.94 (3 H, t, J = 9.0 Hz) (Fig. S7). ^{13}C NMR (151 MHz, $CDCl_3$) δ 190.04, 150.78, 143.47, 131.05, 130.06, 128.43, 127.58, 127.55, 125.06, 123.85, 123.57, 115.96, 114.80, 77.23, 77.02, 76.81, 47.69, 28.84, 20.07, 13.75 (Fig. S8); MS (HR-MS): *m/z* 284.1102 $[M+H]^+$ (Fig. S9, Calcd for $C_{17}H_{17}NOS$: 283.1031); Anal. Calcd. (%) for $C_{17}H_{17}NOS$: C, 72.05; H, 6.05; N, 4.94. Found (%): C, 72.02; H, 6.03; N, 4.96.

2.2.4. 10-Hexyl-10H-phenothiazine-3-carbaldehyde (*PCA6*)

The synthetic method for compound **PCA6** was similar to that of compound **PCA1**. It was purified by column chromatography (silica gel, petroleum ether/CH_2Cl_2 = 1/1) to give yellow solid (75% in yield). mp: 62–64 °C. IR (KBr, cm^{-1}): 1678, 1600, 1576, 1564, 1474, 1450, 1448, 1441, 1369, 1254, 1226, 1200, 752. ^{1}H NMR (600 MHz, $CDCl_3$) δ 9.79 (1 H, s), 7.65–7.63 (1 H, dd, J_1 = 8.4 Hz, J_2 = 1.7 Hz), 7.58 (1 H, d, J = 1.7 Hz), 7.19–7.15 (1 H, m), 7.12–7.10 (1 H, dd, J_1 = 7.6 Hz, J_2 = 1.2 Hz), 6.97–6.95 (1 H, m), 6.90–6.87 (2 H, t, J = 9.2 Hz), 3.89–3.87 (2 H, t, J = 7.2 Hz), 1.83–1.78 (2 H, m), 1.45–1.43 (2 H, t, J = 7.2 Hz), 1.31 (4 H, d, J = 3.4 Hz), 0.88–0.86 (3 H, t, J = 7.2 Hz) (Fig. S10). ^{13}C NMR (151 MHz, $CDCl_3$) δ 190.03, 150.76, 143.46, 131.04, 130.06, 128.42, 127.57, 127.55, 125.03, 123.82, 123.56, 115.95, 114.79, 48.03, 31.38, 26.74, 26.51, 22.56, 13.96. (Fig. S11); MS (HR-MS): *m/z* 312.1413 $[M+H]^+$ (Fig. S12, Calcd for $C_{19}H_{21}NOS$: 311.1344); Anal. Calcd. (%) for $C_{19}H_{21}NOS$: C, 73.27; H, 6.80; N, 4.50. Found (%): C, 73.32; H, 6.83; N, 4.46.

3. Results and discussion

3.1. Photophysical properties in solutions

The UV–vis absorption and fluorescence emission spectra of phenothiazine derivatives **PCA1**, **PCA2**, **PCA4** and **PCA6** in THF ($c = 1.0 \times 10^{-6}$ M) were shown in Fig. 1. It was found that all of the phenothiazine derivatives exhibited three obvious absorption bands, in the region of 280–300 nm was originating from the phenothiazine and localized π-π* transitions [38], and the band appearing at the longer wavelength region of 375–390 nm was mainly ascribed to the charge transfer (CT) from phenothiazine donor to formyl group acceptor. In addition, the maximal emission peaks of **PCA1**, **PCA2**, **PCA4** and **PCA6** in THF emerged at ~507 nm, which was ascribed to CT emission. It could be confirmed by the solvent dependent fluorescence emission spectra (Fig. S13).

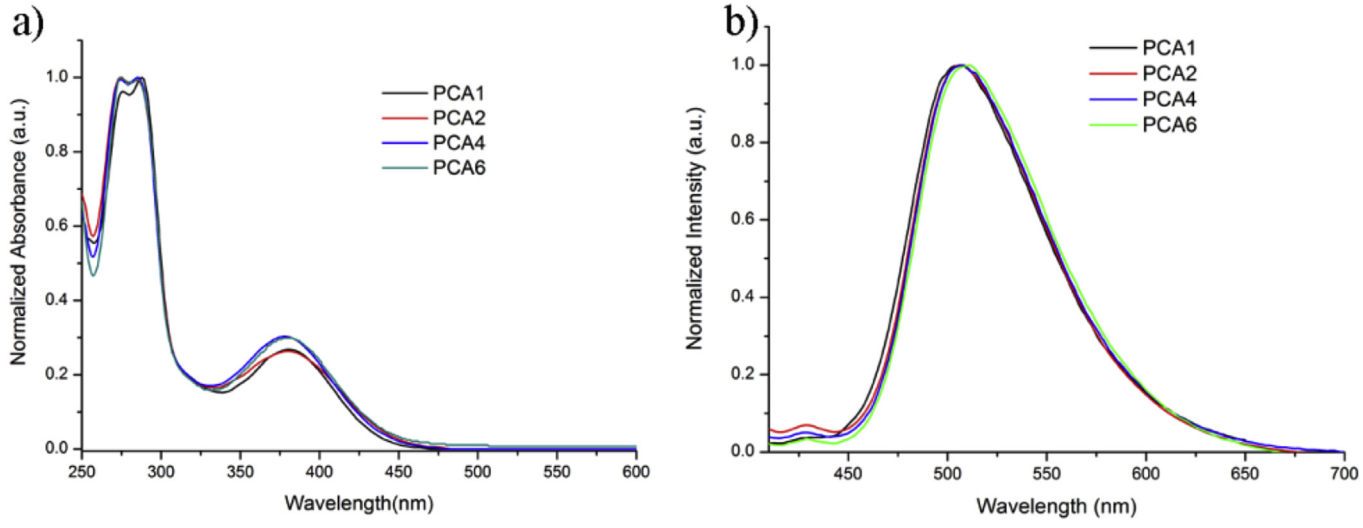

Fig. 1. The UV–vis absorption and fluorescence emission spectra of **PCA1**, **PCA2**, **PCA4** and **PCA6** in THF ($c = 1.0 \times 10^{-6}$ M, λ_{ex} = 410 nm).

Because all the compounds have the same chromophores, **PCA2** was used as the sample. It was clear that the maximal absorption peak was observed at 375 nm in cyclohexane, a red-shifted peak (380 nm) for toluene solution appeared, and the DMF solution possessed an absorption band at 381 nm. The red-shift of the absorption peak in polar solvents suggests that **PCA2** is a polar molecule [39,40], which can be confirmed by quantum chemical calculations. And quantum chemical calculations were performed by time-dependent density functional theory (TD-DFT) calculations at the B3LYP/6-31G (d, p) level and the calculated dipole moment was 5.5458 D, which indicated **PCA2** had large molecular polarity. Moreover, it was found that the fluorescence of **PCA2** also exhibited solvatochromism. A structured emission band with a maximum emission peak at 468 nm and a shoulder peak at 490 nm were observed in cyclohexane. With solvent polarity increasing, the emission bands became structureless and the emission wavelength red-shifted, the maximum emission band of **PCA2** in DMF shifted to 547 nm. Red shifts of the emission wavelength in polar solvents indicated a stronger polarity of **PCA2** in excited state than in ground state. For the other three compounds, similar spectral behaviors were found because of their same chromophores and the detailed data were listed in Table S1 and Table S2.

3.2. Theoretical calculation and electrochemical properties

Considering the molecular structures, PCAn are typical D-A molecules, in which formyl groups act as electron-withdrawing groups, phenothiazine groups are electron donors. Quantum chemical calculations also confirmed this conclusion. After geometry optimization, the absorption spectrum was simulated by the time-dependent DFT calculation at the B3LYP/6-31G (d, p) level. A wide absorption band with a maximum at 411.7 nm was found (Fig. S14), which consisted of one strong and one weak absorption bands. The detailed results were listed in Table S3. The results showed that electron transitions corresponding to absorption bands involve six frontier orbitals (Fig. S15 and Table S3) and the first transition (HOMO→LUMO) will induce charge transfer from phenothiazine to formyl group, which resulted in an excited state with a larger polarity relative to that of the ground state. Furthermore, the twisted angles of phenothiazine group reached 154.2° (Fig. 2a), suggesting a nonplanar molecular conformation. And the frontier orbital plots of the HOMO and LUMO were shown in Fig. 2b and Fig. S16. It was found that the LUMO orbitals were almost

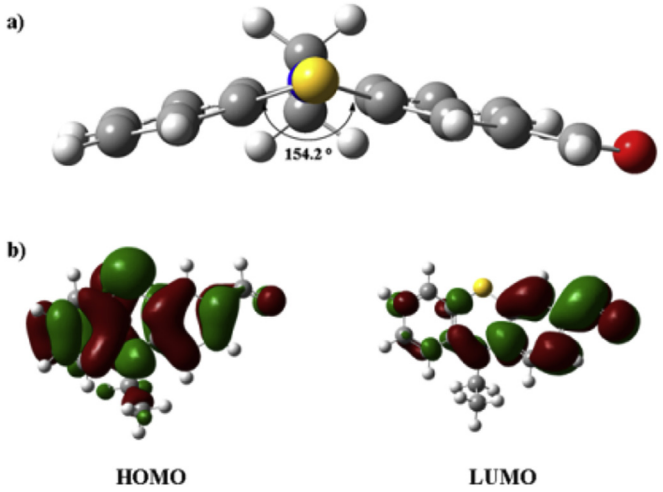

Fig. 2. (a) Optimized molecular structure and (b) electron density distributions of the frontier molecular orbitals of **PCA2**.

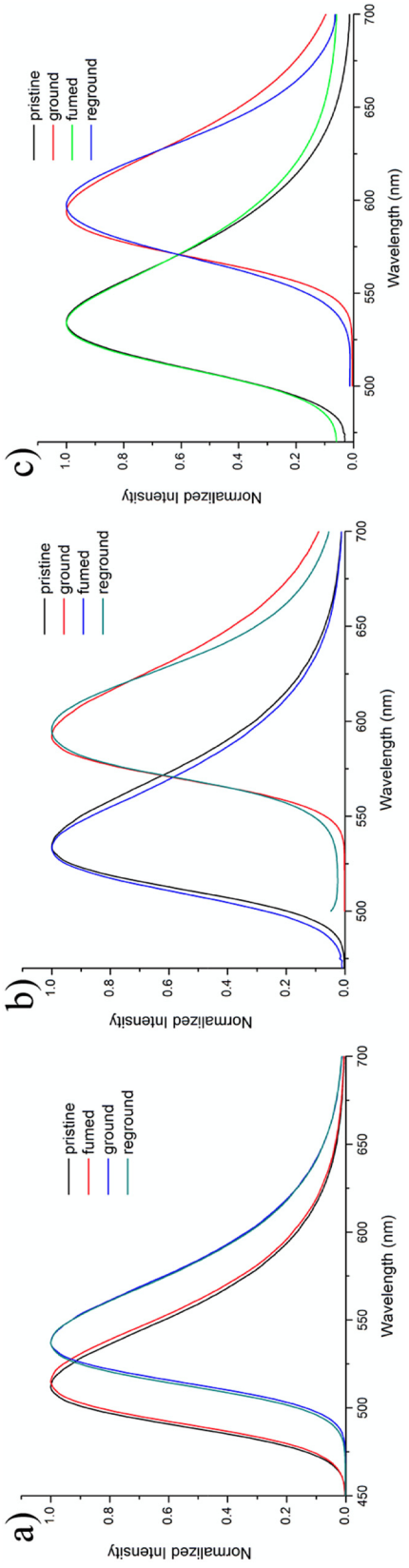

Fig. 3. Normalized solid-state fluorescence spectra of (a) **PCA1**, (b) **PCA2**, and (c) **PCA4** in different states.

Table 1
Peak wavelengths (λ/nm) of PCAn under various external stimuli.

Samples	$\lambda_{annealed}$	$\lambda_{pressed}$	λ_{fumed}	$\lambda_{repressed}$	$\Delta\lambda_{MFC}$[a]
PCA1	515	537	512	537	22
PCA2	535	592	534	594	57
PCA4	533	594	535	596	61

[a] Pressing-induced spectral shift, $\Delta\lambda_{MFC} = \lambda_{pressed} - \lambda_{annealed}$.

distributed at formyl groups and the near benzene rings, while the HOMO orbitals mainly populated predominately on the phenothiazine moieties. Therefore, PCAn are polar molecules and mechanochromic activities were expected for them in the solid states.

To gain insight into the nature of the ground electronic state of these four phenothiazine derivatives PCAn, we performed theoretical calculations on their energy levels by using the density functional theory (DFT) method at B3LYP/6-31G (d, p) basis in the Gaussian 09W program package and cyclic voltammetry (CV) measurements were performed in dry dichloromethane solutions with Tetrabutylammonium Tetrafluoroborate as the supporting electrolyte. Cyclic voltammograms of **PCA1**, **PCA2**, **PCA4** and **PCA6** are shown in Fig. S17, and the corresponding data are listed in Table S2. It was found that all of the phenothiazine derivatives exhibited two well-defined reversible oxidation processes and the half-wave potential located at 1.02, 1.00, 1.02 and 1.02 V (vs. Fc/Fc^+), respectively. The redox potential of Fc/Fc^+ was located at 0.58 eV which possessed an absolute energy level of 4.8 eV relative to the vacuum level for calibration in our case. Additionally, the HOMO energy level was estimated according to the equation of $E_{HOMO} = -(E_{ox} + 4.22)$, and the LUMO energy level was calculated using the empirical equation of $E_{LUMO} = E_{HOMO} + Egap$, in which Egap was estimated from the onset of the absorption spectrum ($Egap = 1240/\lambda onset$). So the HOMO energy levels of PCAn were located at −5.24, −5.22, −5.24 and −5.24 eV, and their LUMO energy levels were located at −2.32, −2.28, −2.34 and −2.34 eV, respectively.

3.3. MFC properties of PCAn

Some non-planar tetraphenylethene, 9,10-divinylanthracene exhibit excellent MFC behavior with high contrast [41,42]. Especially, some functionalized phenothiazine derivatives showed good MFC behaviors which contained a non-planar butterfly conformation. And we have previously reported that some phenothiazine-based compounds exhibited MFC properties [43]. So we predicted that nonplanar D-A typed phenothiazine derivatives PCAn would exhibit MFC behaviors.

To check whether PCAn are mechanochromic, their fluorescence responses toward mechanical and solvent-fuming processes were studied. Fig. S18 and Fig. S19 were the fluorescence images of PCAn samples (mixed with KBr in order to save fluorophores) upon a cycle of pressing, heat-annealing, repressing and solvent-fuming. It was observed that the pressed PCAn samples emit yellowish-green to orange colors from **PCA1** to **PCA4** under UV illumination of a 365 nm lamp. However, when the pressed samples were annealed before the isotropic melt transition or exposed to solvent vapor (fuming above dichloromethane for 60s), green or yellowish-green fluorescence colors appeared again. But this phenomenon did not happen for **PCA6** (Fig. S19 and Fig. S20). It was quite clear that, the PCAn with longer alkyl chains (n = 2, 4) exhibited more remarkable fluorescence color changes between pressed and annealed (or fumed) states (from orange to yellowish-green) than that with shorter alkyl chain (n = 1, from yellowish-green to green). Furthermore, when the fumed or annealed samples were repressed, the fluorescence colors were again changed as the first pressing. This process is reproducible, indicating a reversible MFC

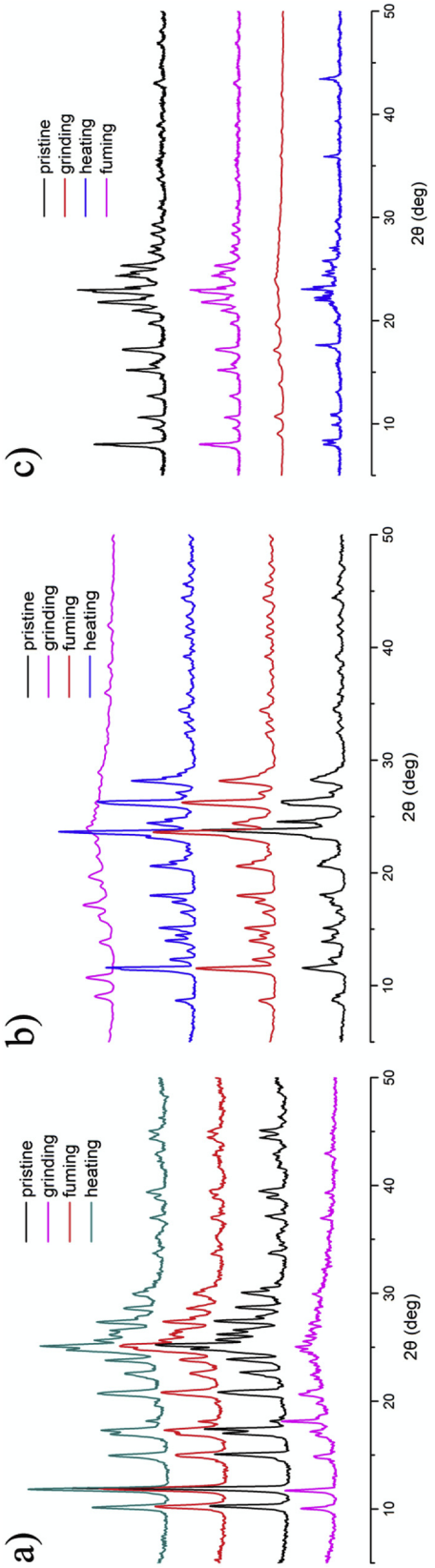

Fig. 4. Powder wide-angle X-ray diffraction patterns of **PCA1** (a), **PCA2** (b) and **PCA4** (c) in different states at room temperature.

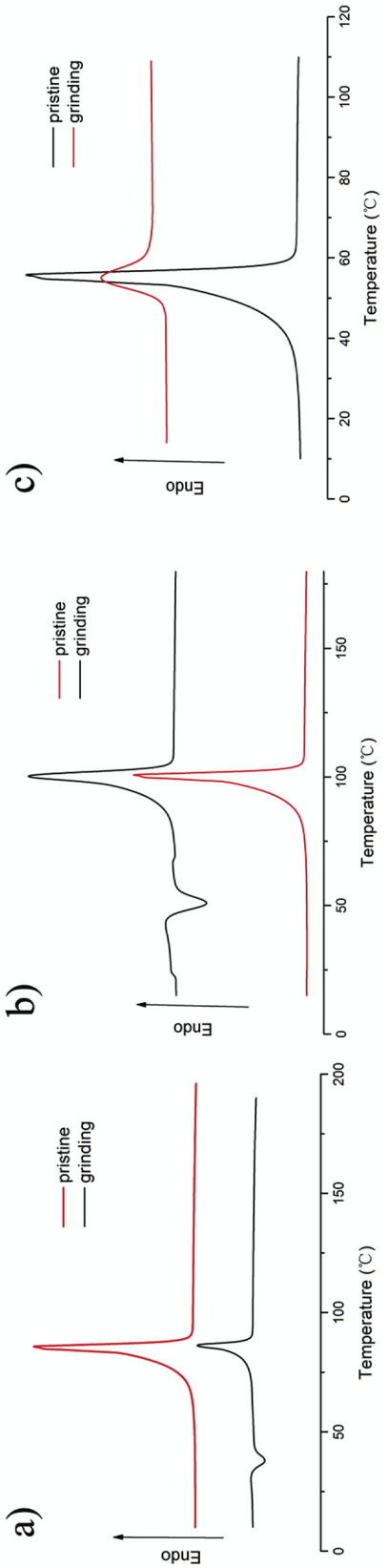

Fig. 5. DSC curves of **PCA1** (a), **PCA2** (b) and **PCA4** (c) under pristine and ground states.

behavior [44]. When the samples were pressed, the red shifts of PCAn fluorescence emission wavelength occurred to some extent. Meanwhile, the emission spectra of above samples under various stimuli were recorded on a luminescence spectrophotometer (Fig. 3), the corresponding spectroscopic data were summarized in Table 1. As expected, the emission spectra recorded are comparably consistent with the corresponding fluorescence colors observed (Fig. S18). It was found that the peak emission wavelengths of pressed PCAn were 537, 592 and 594 nm, respectively, and the maximum emission of annealed states emerged at 515, 535 and 533 nm. Obviously, based on the emission spectra, the general trend of $\Delta\lambda_{MFC}$ ($\Delta\lambda_{MFC} = \lambda$pressed - λannealed) increases with the length of alkyl chains. Therefore, PCAn homologs are also alkyl chain length-dependent MFC materials, and alkyl chains have played a functional role in tuning the MFC behavior [44,45].

To understand what happens upon pressing PCAn sample, powder wide-angle X-ray diffraction (XRD) and differential scanning calorimetry (DSC) experiments were conducted on the ground and as-prepared solids. As shown in Fig. 4, the diffraction curves of as-prepared PCAn solid showed sharper and more intense reflections, indicative of existence of the well-ordered micro-crystalline structures. In contrast, the diffraction peaks of the ground samples displayed broad and weak peaks, indicating notable amorphous features [8]. The diffraction peaks, and hence the crystalline structures, could be recovered after fuming or annealing, which resulted in blue shifts in the fluorescence spectra. The results indicated that the MFC properties of the PCAn solid samples should be attributed to the phase transition between crystalline and amorphous states [46].

The formation of amorphous state upon grinding has been further confirmed by DSC experiment. As shown in Fig. 5, the compounds exhibited obvious melting peak located at 87 °C, 101 °C and 55 °C, for **PCA1**, **PCA2**, and **PCA4**, respectively, and there was no change upon grinding. DSC curves showed that **PCA1** and **PCA2** displayed exothermic transition peak at the lower-temperature region in the ground state at 40 °C and 51 °C. This broad exothermic peak could be ascribed to the cold-crystallization (crystallizing from glass state) of ground PCAn solids upon annealing [47], which confirmed that the amorphous state was a metastable state. Unluckily, **PCA4** gave no phase transition peak in ground state. The ground **PCA2** solids had high exothermic peak values, which resulted in their stable MFC behavior at room temperature. The ground **PCA1** solid could cold-crystallize at room temperature since its exothermic peak was located at 40 °C. Thus, the amorphized **PCA1** solid induced by grinding rapidly recovered its fluorescence at lower temperatures and even exhibited spontaneous recovering fluorescence properties at room temperature.

4. Conclusions

A series of bowl-shaped phenothiazine derivatives functionalized by formyl group (PCAn, n = 1, 2, 4 and 6) with different lengths of *N*-alkyl chains have been designed, The spectral results and quantum chemical calculations indicate that the compounds are D-A molecules. Interestingly, these simple non-planar compounds **PCA1**, **PCA2** and **PCA4** exhibit pronounced and reproducible reversible mechanochromism, not only naked-eye visible and reversible mechanochromic behavior, but alkyl chain length-dependent emission properties. XRD and DSC reveal that the transformation between crystalline and amorphous states upon various external stimuli is responsible for the MFC behavior. This work has demonstrated that the subtle manipulation of alkyl groups of phenothiazine functionalized by formyl group could endow these compounds with unique and tunable solid-state optical properties. And another phenothiazine derivatives are under

research.

Acknowledgment

This work was supported by grants from the Natural Science Foundation of Science and Technology Agency of Shanxi Province (201601D021056), the Natural Science Foundation of Education Committee of Shanxi Province (20161111), and the Doctor Fund of Shanxi Normal University (0505/02070262).

Appendix A. Supplementary data

Supplementary data related to this article can be found at http://dx.doi.org/10.1016/j.dyepig.2017.08.049.

References

[1] Sagara Y, Kato T. Mechanically induced luminescence changes in molecular assemblies. Nat Chem 2009;1:605–10.
[2] Chi ZG, Zhang XQ, Xu BJ, Zhou X, Ma CP, Zhang Y, et al. Recent advances in organic mechanofluorochromic materials. Chem Soc Rev 2012;41:3878–96.
[3] Sagara Y, Kato T. Stimuli-responsive luminescent liquid crystals: change of photoluminescent colors triggered by a shear-induced phase transition. Angew Chem Int Ed 2008;47:5175–8.
[4] Jia JH, Xue PC, Lu R. Stimuli-response fluorescence behaviors of dimesitylboron functionalized with tetraphenylethylene. Tetrahedron Lett 2016;57:2544–8.
[5] Babu SS, Praveen VK, Ajayaghosh A. Functional π-gelators and their applications. Chem Rev 2014;114:1973–2129.
[6] Zhu XL, Liu R, Li YH, Huang H, Wang Q, Wang DF, et al. An AIE-active boron-difluoride complex: multi-stimuli-responsive fluorescence and application in data security protection. Chem Commun 2014;50:12951–4.
[7] Andres J, Hersch RD, Moser J, Chauvin A. A new anti-counterfeiting feature relying on invisible luminescent full color images printed with lanthanide-based inks. Adv Funct Mater 2014;24:5029–36.
[8] Xue PC, Yao BQ, Liu XH, Sun JB, Gong P, Zhang ZQ, et al. Reversible mechanochromic luminescence of phenothiazine-based 10, 10′-bianthracene derivatives with different lengths of alkyl chains. J Mater Chem C 2015;3:1018–25.
[9] Zhang XQ, Chi ZG, Zhang Y, Liu SW, Xu JR. Recent advances in mechanochromic luminescent metal complexes. J Mater Chem C 2013;1:3376–90.
[10] Ma CP, Zhang XQ, Yang LT, Li Y, Liu HL, Yang Y, et al. Alkyl length dependent mechanofluorochromism of AIE-based phenothiazinyl fluorophenyl acrylonitrile derivatives. Dyes Pigments 2017;136:85–91.
[11] Bu LY, Li YP, Wang JF, Sun MX, Zheng M, Liu W, et al. Synthesis and piezochromic luminescence of aggregation-enhanced emission 9, 10-bis (N-alkylcarbazol-2-yl-vinyl-2) anthracenes. Dyes Pigments 2013;99:833–8.
[12] Shan GG, Li HB, Cao HT, Sun HZ, Zhu DX, Su ZM. Influence of alkyl chain lengths on the properties of iridium (III)-based piezochromic luminescent dyes with triazole-pyridine type ancillary ligands. Dyes Pigments 2013;99:1082–90.
[13] Liu W, Wang YL, Bu LY, Li JF, Sun MX, Zhang DT, et al. Chain length-dependent piezofluorochromic behavior of 9, 10-bis (p-alkoxystyryl) anthracenes. J Lumin 2013;143:50–5.
[14] Xue SF, Qiu X, Sun QK, Yang WJ. Alkyl length effects on solid-state fluorescence and mechanochromic behavior of small organic luminophores. J Mater Chem C 2016;4:1568–78.
[15] Ooyama Y, Harima Y. Molecular design of mechanofluorochromic dyes and their solid-state fluorescence properties. J Mater Chem 2011;21:8372–80.
[16] Xu BJ, He JJ, Mu YX, Zhu QZ, Wu SK, Wang YF, et al. Very bright mechanoluminescence and remarkable mechanochromism using a tetraphenylethene derivative with aggregation-induced emission. Chem Sci 2015;6:3236–41.
[17] Xue PC, Ding JP, Wang PP, Lu R. Recent progress in the mechanochromism of phosphorescent organic molecules and metal complexes. J Mater Chem C 2016;4:6688–706.
[18] Xue PC, Sun JB, Chen P, Gong P, Yao BQ, Zhang ZQ, et al. Strong solid emission and mechanofluorochromism of carbazole-based terephthalate derivatives adjusted by alkyl chains. J Mater Chem C 2015;3:4086–92.
[19] Xue PC, Yao BQ, Sun JB, Xu Q, Chen P, Zhang ZQ, et al. Phenothiazine-based benzoxazole derivates exhibiting mechanochromic luminescence: the effect of a bromine atom. J Mater Chem C 2014;2:3942–50.
[20] Xue PC, Chen P, Jia JH, Xu QX, Sun JB, Yao BQ, et al. A triphenylamine-based benzoxazole derivative as a high-contrast piezofluorochromic material induced by protonation. Chem Commun 2014;50:2569–71.
[21] Misra R, Jadhav T, Dhokale B, Mobin SM. Reversible mechanochromism and enhanced AIE in tetraphenylethene substituted phenanthroimidazoles. Chem Commun 2014;50:9076–8.
[22] Gong Y, Zhang Y, Yuan WZ, Sun JZ, Zhang Y. D-A solid emitter with crowded and remarkably twisted conformations exhibiting multifunctionality and multicolor mechanochromism. J Phys Chem C 2014;118:10998–1005.
[23] Sun JB, Sun JB, Mi WH, Xue PC, Zhao JY, Zhai L, et al. Carbazole modified salicylaldimines and their difluoroboron complexes: effect of the tert-butyl and trifluoromethyl terminal groups on organogelation and piezofluorochromism. New J Chem 2017;41:763–72.
[24] Ma CP, Xu BJ, Xie GY, He JJ, Zhou X, Peng BY, et al. An AIE-active luminophore with tunable and remarkable fluorescence switching based on the piezo and protonation-deprotonation control. Chem Commun 2014;50:7374–7.
[25] Cheng X, Li D, Zhang ZY, Zhang HY, Wang Y. Organoboron compounds with morphology-dependent NIR emissions and dual-channel fluorescent ON/OFF switching. Org Lett 2014;16:880–3.
[26] Zhang G, Lu J, Sabat M, Fraser CL. Polymorphism and reversible mechanochromic luminescence for solid-state difluoroboron avobenzone. J Am Chem Soc 2010;132:2160–2.
[27] Zhang G, Singer JP, Kooi SE, Evans RE, Thomas EL, Fraser CL. Reversible solid-state mechanochromic fluorescence from a boron lipid dye. J Mater Chem 2011;21:8295–9.
[28] Yoshii R, Hirose A, Tanaka K, Chujo Y. Boron diiminate with aggregation-induced emission and crystallization-induced emission-enhancement characteristics. Chem -Eur J 2014;20:8320–4.
[29] Luo M, Zhou X, Chi ZG, Liu SW, Zhang Y, Xu JR. Fluorescence-enhanced organogelators with mesomorphic and piezofluorochromic properties based on tetraphenylethylene and gallic acid derivatives. Dyes Pigments 2014;101:74–84.
[30] Lu QY, Li XF, Li J, Yang ZY, Xu BJ, Chi ZG, et al. Influence of cyano groups on the properties of piezofluorochromic aggregation-induced emission enhancement compounds derived from tetraphenylvinyl-capped ethane. J Mater Chem C 2015;3:1225–34.
[31] Sun JB, Sun JB, Mi WH, Xue PC, Zhao JY, Zhai L, et al. Self-assembling and piezofluorochromic properties of *tert*-butylcarbazole-based Schiff bases and the difluoroboron complex. Dyes Pigments 2017;136:633–40.
[32] Jia JH, Cao KY, Xue PC, Zhang Y, Zhou HP, Lu R. Y-shaped dyes based on triphenylamine for efficient dye-sensitized solar cells. Tetrahedron 2012;68:3626–32.
[33] Jia JH, Xue PC, Zhang Y, Xu QX, Zhang GH, Huang TH, et al. Fluorescent sensor based on dimesitylborylthiophene derivative for probing fluoride and cyanide. Tetrahedron 2014;70:5499–504.
[34] Xue PC, Ding JP, Chen P, Wang PP, Yao BQ, Sun JB, et al. Mechanical force-induced luminescence enhancement and chromism of a nonplanar D-A phenothiazine derivative. J Mater Chem C 2016;4:5275–80.
[35] Ma CP, Zhang XQ, Yang Y, Ma ZY, Wu YJ, Liu HL, et al. Halogen effect on mechanofluorochromic properties of alkyl phenothiazinyl phenylacrylonitrile derivatives. Dyes Pigments 2016;129:141–8.
[36] Sun JW, Dai YY, Ouyang M, Zhang YJ, Zhan LL, Zhang C. Unique torsional cruciform π-architectures composed of donor and acceptor axes exhibiting mechanochromic and electrochromic properties. J Mater Chem C 2015;3:3356–63.
[37] Zhang GH, Sun JB, Xue PC, Zhang ZQ, Gong P, Peng J, et al. Phenothiazine modified triphenylacrylonitrile derivates: AIE and mechanochromism tuned by molecular conformation. J Mater Chem C 2015;3:2925–32.
[38] Hua Y, Chang S, Huang DD, Zhou X, Zhu XJ, Zhao JZ, et al. Significant Improvement of Dye-sensitized solar cell performance using simple phenothiazine based dyes. Chem Mater 2013;25:2146–53.
[39] Xue PC, Xu QX, Gong P, Qian C, Zhang ZQ, Jia JH, et al. Two-component gel of a D-π-A-π-D carbazole donor and a fullerene acceptor. RSC Adv 2013;3:26403–11.
[40] Xue PC, Yao BQ, Liu XH, Sun JB, Gong P, Zhang ZQ, et al. Reversible mechanochromic luminescence of phenothiazine-based 10, 10′-bianthracene derivatives with different lengths of alkyl chains. J Mater Chem C 2015;3:1018–25.
[41] Zhang XQ, Chi ZG, Li HY, Xu BJ, Li XF, Zhou W, et al. Piezofluorochromism of an aggregation-induced emission compound derived from tetraphenylethylen. Chem Asian J 2011;6:808–11.
[42] Liu MY, Zhai L, Sun JB, Xue PC, Gong P, Zhang ZQ, et al. Multi-color solid-state luminescence of difluoroboron β-diketonate complexes bearing carbazole with mechanofluorochromism and thermofluorochromism. Dyes Pigments 2016;128:271–8.
[43] Jia JH, Wu YY. Synthesis, crystal structure and reversible mechanofluorochromic properties of a novel phenothiazine derivative. Dyes Pigments 2017;136:657–62.
[44] Zheng M, Sun MX, Li YP, Wang JF, Bu LY, Xue SF, et al. Piezofluorochromic properties of AIE-active 9,10-bis(N-alkylphenothiazin-3-yl-vinyl-2)anthracenes with different length of alkyl chains. Dyes Pigments 2014;102:29–34.
[45] Zhang XQ, Chi ZG, Zhang JY, Li HY, Xu BJ, Li XF, et al. Piezofluorochromic properties and mechanism of an aggregation-induced emission enhancement compound containing N-Hexyl-phenothiazine and anthracene moieties. J Phys Chem B 2011;115:7606–11.
[46] Zhang XQ, Chi ZG, Xu BJ, Jiang L, Zhou X, Zhang Y, et al. Multifunctional organic fluorescent materials derived from 9,10-distyrylanthracene with alkoxyl endgroups of various lengths. Chem Commun 2012;48:10895–7.
[47] Vasanthan N, Jyothi Manne N, Krishnama A. Effect of molecular orientation on the cold crystallization of amorphous-crystallizable polymers: the case of poly (trimethylene terephthalate). Ind Eng Chem Res 2013;52:17920–6.